Functionalisation of MWCNTs with poly(lauryl acrylate) polymerised by Cu(0)-mediated and RAFT methods†

Jaipal Gupta,[a] Daniel J. Keddie,[b] Chaoying Wan,[a] David M. Haddleton[c] and Tony McNally*[a]

[a.] *International Institute for Nanocomposites Manufacturing (IINM), WMG, University of Warwick, CV4 7AL, UK. E-mail: t.mcnally@warwick.ac.uk*
[b.] *School of Biology, Chemistry and Forensic Science, University of Wolverhampton, WV1 1LY, UK.*
[c.] *Department of Chemistry, University of Warwick, Library Road, Coventry, CV4 7AL, UK.*
†Electronic Supplementary Information (ESI) available: ^{1}H NMR spectra of compound **A**; TGA of LA and cyanomethyl dodecyltrithiocarbonate. See DOI: 10.1039/x0xx00000x

Poly(lauryl acrylate) P[LA] of various molar masses were prepared *via* reversible addition-fragmentation chain transfer (RAFT) polymerisation and Cu(0)-mediated radical polymerisation for the purpose of improving the dispersion and interfacial adhesion of MWCNTs with polymers such as isotactic poly(propylene) (iPP). Lauryl acrylate (LA) polymerised *via* RAFT to high conversion (95%), furnished polymers in good agreement with theoretical M_n with dispersity increasing with increasing M_n. LA polymerised *via* the Cu(0)-mediated method to full conversion (>98%), gave polymers in good agreement with theoretical M_n and low dispersity ($Đ$; ≈ 1.2) for lower molar mass polymers. Low molar mass termination was also observed for P[LA] *via* Cu(0)-mediated polymerisation for higher molar mass polymers. Thermogravimetric analysis (TGA) of P[LA] *via* RAFT showed an onset of degradation occurred at ≈ 340 – 350 °C, however, this decreased to ≈ 250 – 260 °C for lower molar mass polymers. TGA of the RAFT agent revealed an onset of degradation of ≈ 200 – 250 °C. Free radicals generated from thermal degradation of end groups does not influence the thermal stability of P[LA] backbone and 'unzipping' commonly seen with methacrylates was not observed. TGA analysis of P[LA] *via* the Cu(0)-mediated method revealed a similar degradation profile to that of P[LA] *via* RAFT. The thermal stability of P[LA] is sufficient to allow for melt processing with iPP. P[LA] *via* RAFT mixed with MWCNTs showed an adsorption of ≈ 10 – 25 wt% P[LA] on to the MWCNTs. The onset of thermal degradation of the P[LA] remained unchanged after adsorption on to the MWCNTs. P[LA] *via* the Cu(0)-mediated method adsorbed up to 85 wt% and an increase in thermal stability of ≈ 50 °C was recorded. Increasing P[LA] and MWCNT concentration independently also resulted in an increase in the level of adsorption, possibility due to increased CH-π interaction. The difference in thermal stability could possibly be due to heat transfer from the P[LA] to the MWCNTs, resulting in delayed pyrolysis of P[LA]. Size exclusion

chromatography (SEC) and matrix-assisted laser desorption/ionization time of flight mass spectrometry (MALDI-TOF MS) of P[LA] after heating to 200 °C for 30 mins in air showed loss of end groups but, the P[LA] backbone remained preserved for both polymer types. Evidence from transmission electron micrographs (TEM) shows the P[LA] adsorbing onto the MWCNT surface. Melt processing composites of P[LA] *via* Cu(0)-mediated with MWCNTs and iPP was possible as the P[LA] was thermally stable during the both extrusion and in the TGA when studied post melt mixing.

Introduction

A detailed understanding of the thermal and thermo-mechanical stability of polymers synthesised using reversible deactivation radical polymerisation (RDRP) techniques that can be used for melt processing, e.g. extrusion and injection moulding is limited.[1, 2] RDRP techniques have effectively established the synthesis of well-defined polymers of targeted molar mass and low molar mass dispersity with complex architecture and specific functionality.[3] However, melt processing of such polymers has been limited due to a lack of understanding regarding the thermo-mechanical stability of the resulting polymers as a consequence of being subjected to high shear stresses and temperature during melt processing.[1] In order to significantly expand the use of tailored polymers prepared using RDRP methods that could be exploited industrially, a detailed understanding of the effects of stress and temperature applied during processing on polymer structure is critically required.

Atom transfer radical polymerisation (ATRP)[4], nitroxide-mediated polymerisation (NMP)[5] and reversible addition-fragmentation chain transfer (RAFT) polymerisation[6-9] are currently popular RDRP methods. It has been demonstrated that Cu(0)-mediated polymerisation is highly efficient in allowing facile synthesis of well-defined, high molar mass polymers at ambient temperatures with low molar mass dispersity whilst retaining high end group fidelity.[10-12] In particular, Cu(0)-mediated polymerisation has shown to provide impressive control of monomers containing long hydrophobic side chains e.g. lauryl acrylate.[13, 14] Copper (Cu) catalysed radical polymerisation is finding increased applications in industry as it can be used in a wide range of monomer/solvent systems as well as being more tolerant to the presence of impurities and oxygen.[15] Additionally, it has been shown that RAFT is highly adaptable and effective at polymerising a large range of monomer types in a wide range of solvents with superior control over molar mass and dispersity for a variety of molecular architectures.[16] A significant advantage of RAFT over alternate RDRP methods from an industry standpoint is the minimal deviation from standard radical polymerisation protocols; the

methodology need only be altered solely through addition of the RAFT agent. Furthermore RAFT uses no transition metal species, thus issues associated with subsequent catalyst removal is mitigated entirely.

It is important to consider the effects of thermal and mechanical stress on the molecular structure of functional polymers as their ability to withstand both during the melt mixing process will enable their use, by way of example, for improving the compatibilisation of carbon nanotubes (CNTs) with thermoplastic polymers, such as isotactic poly(propylene)(iPP).

Whilst thermolysis has been applied as a method for transformation of functional chain-ends,[17, 18] limited work has been carried out with respect to understanding the effects of high shear and temperature during processing of polymers synthesised using RDRP methods. Altintas *et al.* has shown that the molar mass of trithiocarbonate mid-chain functional polymers decreased at elevated temperatures (200 °C) whereas, trithiocarbonate end-functional polymers resisted thermal degradation under similar conditions.[19] They also showed star-shaped poly(styrenes) with a trithiocarbonate moiety are more susceptible to thermal degradation compared to their linear analogues.[20]

Since the successful identification and characterisation of CNTs by Iijima,[21] their potential use across various applications, such as in electronic devices, energy storage and conversion and, nanocomposites has grown greatly.[22] The remarkable properties of CNTs (e.g. mechanical, thermal and electrical) make them excellent functional fillers for thermoplastics.[23, 24] Their high aspect ratio brings the possibility of significant reinforcement of polymer matrices at very low loadings. Limited solubility with solvents and strong van der Waals interactions between CNTs leads to strongly bound agglomerates, the disentanglement of which has hindered development and application of composites of polymers and MWCNTs.[25] The limiting factor in preventing the widespread application of such materials remains the poorly controlled dispersion and distribution of CNTs within the polymer matrix and poor understanding of the interface and interphase between the CNTs and polymer matrix.[26]

Various methods have been employed to promote compatibilisation between CNTs and polymers including free radical polymerisation techniques to graft polymers to and from CNTs.[27] Covalent attachment of polymers to and from functional groups on the surface of CNTs has been attempted to try and overcome the challenge of poor interfacial interaction between CNTs and many polymer matrices. Covalent attachment can be facilitated by making use of the intrinsic or induced nanotube-bound carboxylic acid groups.[28] A non-oxidative approach using radical chemistry can be used as an alternative to preserve the conjugation length of the CNTs compared to the oxidative approach which results in scission of the CNTs and considerable defect formation[27].

Daugaard *et al.* showed it was possible to polymerise lauryl and stearyl acrylate from the surface of MWCNTs using surface initiated ATRP (SIATRP).[27] Qin *et al.* polymerised *n*-butyl methacrylate from the surface of SWCNTs also using SIATRP.[29] In addition, Wu *et al.* polymerised *n*-butyl acrylate using SIATRP by first functionalising the surface of SWCNTs with an ATRP initiator with subsequent polymerisation. The authors also used atomic force microscopy (AFM) to characterise the overall grafting density and chain-length uniformity.[30] SIATRP (graft from) facilitates a high grafting density however, control of molar mass, dispersity and molecular architecture is limited due to steric hindrance. Adronov *et al.* polymerised styrene using ATRP and grafted this to the surface of SWCNTs using a Cu(I) catalysed azide-alkyne [3 + 2] cycloaddition (CuAAC).[31] The 'graft to' approach enables specific control of polymer architecture but limits grafting density due to sterics from chains giving a mushroom like coverage as opposed to a brush type architecture.

Critically it should be noted, adding any covalent functionality to the surface of CNTs inevitably alters their mechanical and electronic properties. Covalent functionalisation changes the carbon to carbon bonding, i.e. the ratio of sp^2 to sp^3 hybridisation, leading to a partial loss of conjugation, defect creation and ultimately CNT distruction.[32] Non-covalent functionalisation of CNTs preserves their inherent properties, while improving dispersion and interfacial adhesion with polymers. For example, aromatic compounds employ π-π stacking and hydrophobic interactions to bind to the surface of CNTs.[33] Pyrene and porphyrin derivatives have shown to be efficient at adsorbing on the surface of CNTs *via* π-π interactions. Meuer *et al.* synthesised pyrene functionalised poly(methyl methacrylate) (PMMA) *via* RAFT (PMMA-*b*-pyrene) to achieve efficient dispersion and stability in various solvents.[34] Additionally, the use of surfactants for CNT solubilisation in various solvents has received great interest as long hydrophobic chains are readily adsorbed onto the CNT surface.[35] The use of conjugated polymers such as poly(thiophenes) to functionalise CNTs for electronic applications has grown greatly over the last decade.[36] Additionally Yu *et al.* reported the use of RAFT to synthesise a diblock architecture of poly(ethylene glycol) methyl ether acrylate and poly(acrylic acid) and made use of the hydrophobic acrylate backbone to coat the surface of CNTs showing improved dispersion and stability in aqueous media.[37] A combination of π-π stacking and hydrophobic adsorption can drive self-assembly of the polymer around the CNT in the form of wrapping. Even though wrapping is entropically unfavourable, the reduction in surface energy of CNTs in the dispersion media makes the wrapping process thermodynamically favourable.[38]

Herein, we investigate the non-covalent wrapping of poly(lauryl acrylate) P[LA] over MWCNTs, scheme 1. We compare the thermal stability of P[LA] synthesised by both Cu(0) mediated[39] and RAFT[40] polymerisation by TGA, supported by size exclusion chromatography (SEC),

matrix-assisted laser desorption/ionization mass spectrometry (MALDI-TOF MS) and transmission electron microscopy (TEM). The thermal stability of polymers synthesised using different polymerisation techniques has not been reported regularly[41] and therefore, we also look to compare how the two different polymerisation techniques affect the stability of a poly(acrylate). P[LA] is a typical hydrophobic poly(acrylate) and has been shown to co-crystallise with many poly(olefin)s such as iPP.[42] The thermal stability of P[LA] required for melt processing was investigated so as to establish its possible application for compatibilisation with iPP *via* melt extrusion. To the best of our knowledge, there exists no previous study comparing the thermal stability of a polymer synthesised using both Cu(0) mediated and RAFT using a range of techniques.

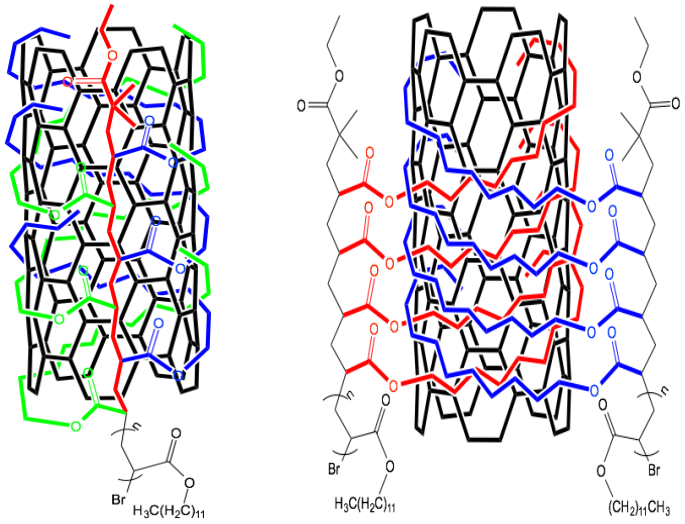

Scheme 1. Schematic representation of P[LA] wrapping around/on a CNT.

Experimental

Materials

1-Dodecanethiol, anhydrous tetrahydrofuran, potassium tert-butoxide, carbon disulfide, chloroacetonitrile, chloroform, sodium chloride, sodium sulfate, ethyl acetate, n-hexane, trimethylamine, ethyl 2-bromoisobutyrate, copper(II) bromide, anhydrous toluene, 2,2'-azobis(2-methylpropionitrile) [AIBN] and isopropanol (IPA) were purchased from Sigma Aldrich or Fisher Scientific and were all used as received. The lauryl acrylate (LA) was purchased from Sigma Aldrich and passed through a column of basic alumina prior to use in order to remove inhibitors. Cu(0)-wire (gauge 0.25 mm) was purchased from Comax Engineering Wires and was treated by immersion in conc. HCl prior to use. *Tris*-(2-(dimethylamino)ethyl)amine (Me_6TREN) was synthesised following the previously published procedure,[43] degassed and stored in a fridge under nitrogen prior to use. Non-functionalised commercially available multi-walled carbon nanotubes (MWCNTs) with an average

diameter of 9.5 nm and average length of 1.5 μm (grade NC7000) were purchased from Nanocyl S. A., Belgium) and used as received. The bulk density was reported to be 66 kg m^{-3} [44] and the oxygen to carbon ratio reported to be 0.0045[45]. Filter paper was obtained from Fisher (cellulose) with a pore size of 20-25 μm. Isotactic poly(propylene) (iPP) with a melt-flow rate of 52 g/10 min (230 °C/ 2.16 kg) (grade H734-52RNA) was purchased from Braskem and used as received.

Synthesis of Cyanomethyl dodecyltrithiocarbonate

1-Dodecanethiol (12.75 g, 63 mmol, 1 eq) was dissolved in 100 mL dry THF. Potassium tert-butoxide (7.07 g, 63 mmol, 1 eq) was added to the solution with stirring at ambient temperature. The solution became thick and cloudy. After stirring for 15 minutes, carbon disulfide, CS_2 (9.6 g, 126 mmol, 2 eq) was added and the solution stirred for a further 30 minutes. Subsequently, chloroacetonitrile (4.75 g 63 mmol, 1 eq) was added and the mixture stirred for a further 24 hours. The solution was diluted with deionised water and extracted with chloroform (3 × 100 mL), washed with brine (2 × 100 mL) and dried with sodium sulphate. The product was then filtered and the solvent removed under reduced pressure. The crude product was purified by column chromatography through silica eluting with 1:9 ethyl acetate/n-hexane. The product was re-crystallised with n-hexane to give the desired product cyanomethyl dodecyltrithiocarbonate (19.22 g, 60 mmol, 96 %). ^{1}H NMR ($CDCl_3$, 400 MHz, 298 K), δ (ppm): 4.16 (s, 2H, -C***H***$_2$-CN), 3.42 (t, J = 7.34 Hz, 2H, -CH_2-C***H***$_2$-S(C=S)S), 1.73 (m, 2H, -C***H***$_2$-CH_2-S(C=S)S), 1.5-1.2 (m, 18H, CH_3-(C***H***$_2$)$_9$-CH_2-) 0.89 (t, J = 6.70 Hz, 3H, C***H***$_3$-$(CH_2)_9$-CH_2-). ^{13}C NMR ($CDCl_3$, 400 MHz, 298 K), δ (ppm): 218.8, 114.7, 38.0, 31.9, 29.6, 29.5, 29.4, 29.3, 29.0, 28.9, 27.8, 22.7, 21.3, 14.1. IR (neat) (cm^{-1}): 2900 (C-H), 2850 (C-H), 2250 (C≡N), 1460, 1370, 1075 (S-(C=S)-S), 850, 810, 720. HRMS (ESI) m/z ($C_{15}H_{27}S_3N$ [M+H^+] requires 318.13) observed 318.14. The data concurs with that reported by Chong *et al.*[46]

Typical RAFT polymerisation procedure

The procedure for RAFT polymerization of lauryl acrylate was adapted from a previously reported literature method.[40] Cyanomethyl dodecyltrithiocarbonate (RAFT agent) (63.5 mg, 0.2 mmol, 1.0 mol equiv.), lauryl acrylate (LA, 2.26 mL, 8.32 mmol, 42.0 mol equiv.), 2,2'-azobis(2-methylpropionitrile) (AIBN, 0.3 mg, 2 μmol, 0.01 mol equiv.) and a magnetic stir bar were charged to a polymerisation Schlenk tube and dissolved in 3 mL of anhydrous toluene. A rubber septum was used to seal the Schlenk tube and the mixture degassed *via* sparging with argon for 20 min. The Schlenk tube was placed in an oil bath heated at 60 °C for 24 h. Toluene was removed using reduced pressure and then the polymer was precipitated by the addition of cold methanol and water (4:1 v/v) from chloroform. Samples of the reaction mixture were carefully removed at the end of the

polymerisation for ^{1}H NMR, mass spectroscopy and GPC analyses. The samples for ^{1}H NMR spectroscopy were diluted in $CDCl_3$, while samples for GPC and MS were diluted with chloroform.

Typical Cu(0)-mediated polymerisation procedure

Poly(lauryl acrylate) was synthesised using the procedure described by Anastasaki *et al*.[39] Ethyl 2-bromoisobutyrate (EBiB, 0.029 mL, 0.20 mmol, 1.00 mol equiv.), lauryl acrylate (LA, 2.26 mL, 8.32 mmol, 42.0 mol equiv.), Me_6TREN (0.064 mL, 0.02 mmol, 0.12 mol equiv.), $CuBr_2$ (2.2 mg, 0.01 mmol, 0.05 mol equiv.), IPA (5 mL) and a magnetic stir bar were charged to a polymerisation Schlenk tube with a rubber septum and the mixture degassed *via* sparging with argon for 15 min. A slight positive pressure of argon was applied and the pre-activated copper wire (4 cm) was then added under an argon blanket. The Schlenk tube was then resealed and the polymerisation proceeded for 24h at ambient temperature. Samples of the reaction mixture were carefully removed at the end of the polymerisation for ^{1}H NMR, MS and GPC analyses. The samples for ^{1}H NMR spectroscopy were diluted in $CDCl_3$, while those for GPC and MS were diluted with chloroform and then passed through a column of basic alumina to remove the copper salts. The poly(lauryl acrylate) P[LA] was precipitated by the addition of cold methanol and water (4:1 v/v) from chloroform to remove copper salts.

Typical protocol for solution mixing of MWCNTs with P[LA]

MWCNTs [50 mg (5 wt%) and 100 mg (10 wt%)] were dispersed in chloroform (100 mL) *via* ultrasonication for 3 minutes at ambient temperature. Subsequently, 1 g of P[LA] was added to the dispersion and the mixture was again sonicated for 3 mins. A magnetic stirrer bar was added to the reaction vessel and the mixture stirred vigorously for 1 hour. The mixture was filtered using a Buchner funnel. The filter cake was collected and dried overnight in a vacuum oven at ambient temperature.

Nanocomposite preparation

The iPP pellets were ground into a powder, using a SPEX® SamplePrep Freezer Mill (Stanmore, UK). The pellets (25 g batch) were pre-cooled for 12 mins followed by two 5 min grinding cycles at 15 Hz. Between each cycle, the sample was cooled for a 2 min interval. The iPP powder was dried in a vacuum oven at 30 °C for 12 h prior to processing. Composites were prepared by dry blending the iPP powder with a given ratio of MWCNTs (0.01, 0.1, 0.3, 0.5, 1, 3 and 5 wt %). The pre-blend was then fed into a Haake™ Mini-Lab II micro-compounder (Thermo-Scientific Haake™) fitted with two conical co-rotating screws and a chamber volume of 5 cm^3. The composite mix was processed for 5

mins at 80 rpm and 165 °C (conditions previously optimised for pure iPP in a control experiment). After 5 mins. The nanocomposite was extruded through a 3.90 x 1.20 mm rectangular die directly into the hot melt chamber of a micro-injection moulding machine (Thermo-Scientific Haake™ MiniJet Pro). Similar procedure was followed for the preparation of composites of iPP and P[LA] functionalised MWCNTs for the same weight fractions.

Characterisation

^{1}H and ^{13}C NMR spectra were recorded on a Bruker DPX-400 spectrometer in $CDCl_3$. Chemical shifts are given in ppm downfield from the internal standard of tetramethylsilane. Size exclusion chromatography (SEC) measurements were conducted using an Agilent 1260 GPC-MDS fitted with differential refractive index (DRI), light scattering (LS), and viscometry (VS) detectors equipped with 2 x PLgel 5 mm mixed D-columns (300 x 7.5 mm), 1 x PLgel 5 mm guard column (50 x 7.5 mm) and autosampler. Low molar mass linear poly(methyl methacrylate) standards in the range 200 to 1.0 x 10^6 g mol^{-1} were used to calibrate the system. All samples were passed through a 0.45 μm PTFE filter prior to analysis. The eluent was chloroform with 2% trimethylamine at a flow rate of 1.0 mL min^{-1}. SEC data was analysed using Cirrus v3.3. MALDI-TOF-MS was conducted using a Bruker Daltonics Ultraflex II MALDI-TOF mass spectrometer, equipped with a nitrogen laser delivering 2 ns laser pulses at 337 nm with positive ion ToF detection performed using an accelerating voltage of 25 kV. Solutions in tetrahydrofuran (50 μL) of *trans*-2-[3-(4-tert-butylphenyl)-2-methyl-2-propyldene] malonitrile (DCTB) as a matrix (saturated solution), sodium iodide as cationization agent (1.0 mg mL^{-1}) and sample (1.0 mg mL^{-1}) were mixed, and 0.7 μL of the mixture was applied to the target plate. Spectra were recorded in reflector mode calibrating PEG-Me 1100 KDa. Thermogravimetric analysis (TGA) was carried out using a Mettler Toledo TGA1-STARe system under the flow of nitrogen (100 cm^3/min). The sample weights ranged from 10-15 mg and were loaded into 70 μL alumina pans. The samples were heated from ambient temperature to 800 °C at a constant heating rate of 10 K min^{-1}. Solutions of MWCNTs mixed with P[LA] were sonicated using a Fisher ultrasonic bath (S30H) at 50 Hz, 280 W.

Results and Discussion

Analysis of the thermal stability of polymers synthesised using RDRP techniques and their possible uses for CNT functionalisation and subsequent use in polymer processing has received little attention to date. The non-covalent approach of CNT functionalisation has yet to be fully explored, especially when considering the use of RDRP polymers for non-covalent functionalization of carbon based 1D and 2D materials. Before the use of RDRP polymers in polymer processing e.g. extrusion

and injection moulding, can be considered, their ability to withstand the thermal and mechanical stresses applied during processing needs to be assessed.

By way of example, poly(lauryl acrylate) was selected based upon its good compatibility with iPP, and because its hydrophobic chains are known to be able to co-crystallise with iPP,[27] a versatile thermoplastic with a wide range of applications. The polymerisation of Lauryl acrylate (LA) was carried out using RAFT[47] and Cu(0)-mediated polymerisation [39]. LA was polymerised using cyanomethyl dodecyltrithiocarbonate RAFT agent. The RAFT agent was prepared via alkylation of a dodecylcarbodithioate salt[16] with chloroacetonitrile, adapting the synthesis method described by Chong *et al*.[46] The ^{1}H NMR for cyanomethyl dodecyltrithiocarbonate is given in Fig. S1 and shows the RAFT agent can be accessed *via* this route in high purity. Additionally the RAFT agent was obtained with improved yield (98%). The adapted synthesis method involved the use of the non-nucleophilic base potassium *tert*-butoxide in place of sodium hydride (NaH). Potassium *tert*-butoxide has been previously shown to deliver greatly improved results in comparison to other strong bases, by simplified work up due to the incidence of fewer undesired side reactions.[16, 48] Initially, lauryl acrylate was polymerised using RAFT (Scheme 2) and Cu(0) mediated polymerisation (Scheme 3). The polymerisation of lauryl acrylate [LA] has been previously reported by Chen *et al*[49] and the polymerisation of long, hydrophobic chain acrylates has also been reported.[40] RAFT polymerisation of LA in toluene gave poly(lauryl acrylate) (P[LA]) with a range of targeted degrees of polymerisation (DP_n = 25, 50 and 100, $M_{n,th}$ = 6,000 – 24,000 g mol^{-1}). ^{1}H NMR (Fig. S2) and SEC analysis (Fig. 1) revealed the polymerisations achieved good conversion (95%) and were in good agreement with theoretical M_n however, dispersity increased with increasing M_n, (Table 1).

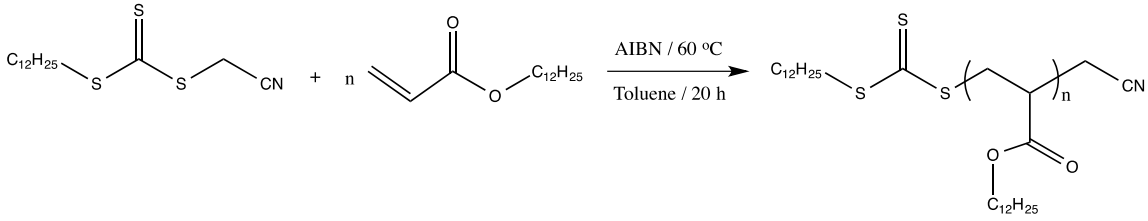

Scheme 2. Synthetic strategy for polymerisation of LA *via* RAFT.

Table. 1 Reaction conditions used for the preparation of initial polymers of LA *via* RAFT polymerisation process and the associated number average molar masses.

Nomenclature	[LA]/[RAFT]	Conv.[a] [%]	$M_{n,\,th}$ [g mol^{-1}]	$M_{n,\,GPC}$[b]	$Đ$[b]
A	25	95	6,000	5,300	1.11
B	50	95	12,000	13,800	1.24
C	100	90	24,000	21,500	1.30

[a] ^{1}H NMR. [b] $CHCl_3$ SEC analysis *via* RI detection using linear PMMA standards.

The polymerisation of LA *via* RAFT proceeded with high conversion as characterised by ^{1}H NMR (Fig. S2). The molar mass and dispersity was characterised by SEC (Fig. 1). SEC analysis shows a linear increase in M_n with increasing monomer to RAFT agent ratio, expressing good control. Low molar mass termination can be observed for the higher molar mass polymers, suggesting further optimisation may be required.

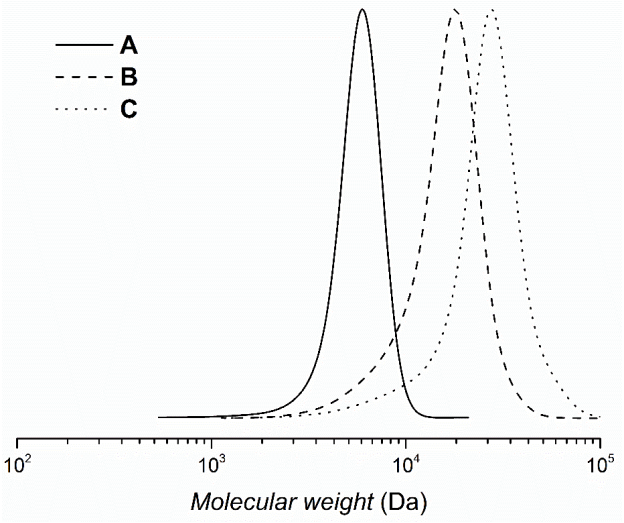

Fig. 1 SEC traces of P[LA] synthesised *via* RAFT polymerisation . P[LA] (**A-C**) defined in table 1.

Cu(0)-mediated homo-polymerisation of LA in IPA as solvent was carried out using the procedure described by Anastasaki *et al.* (Scheme 3). P[LA] with three different degrees of polymerisation (DP = 25, 50 and 100, $M_{n,th}$ = 6,000 – 24,000 g mol^{-1}) were synthesised.[39] ^{1}H NMR (Fig. S3) and SEC analysis (Fig. 2) revealed the polymerisations achieved excellent conversion (>98%), in good agreement with the theoretical M_n and low dispersity ($Đ$; ≈1.2; Table 2).

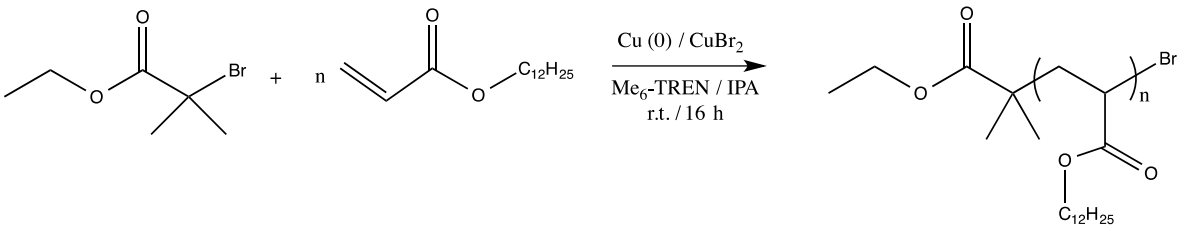

Scheme 3. Synthetic strategy for polymerisation of LA *via* Cu(0) mediated polymerisation .

Table. 2 Reaction conditions used for the preparation of initial polymers of LA *via* Cu(0)-mediated polymerisation process and the associated number average molar masses.

Nomenclature	[LA]/[I]	Conv.[a] [%]	$M_{n,\,th}$ [g mol^{-1}]	$M_{n,\,GPC}$[b] [g mol^{-1}]	$Đ$[b]
D	25	98	6,000	5,500	1.14
E	50	97	12,000	11,900	1.17
F	100	95	24,000	17,500	1.25

[a] ^{1}H NMR. [b] $CHCl_3$ SEC analysis *via* RI detection using linear PMMA standards.

^{1}H NMR of P[LA] (Fig. S3) indicates the polymerisation proceeded to high conversion (≈98%). SEC analysis (Fig. 2) reveals the linear increase in molar mass with increasing monomer to initiator concentration. Low molar mass termination can also be observed causing broadening of dispersity for the higher molar mass polymers.

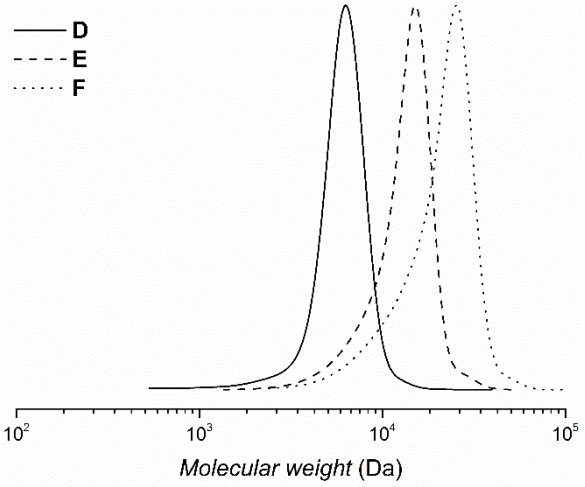

Fig. 2 SEC traces of P[LA] synthesised *via* Cu(0)-mediated polymerisation . P[LA] (**D-F**) defined in table 2.

Thermogravimetric analysis (TGA) was subsequently carried out to investigate the thermal stability of P[LA] and thus its applicability for melt processing. TGA analysis (Fig. 3a) of P[LA] synthesised *via* RAFT showed the onset of degradation occurred at ≈340 - 350 °C with 95 % mass loss by ≈440-450 °C for homopolymers **B** and **C**. Homopolymer **A**, the lowest molar mass polymer shows an earlier onset of degradation at ≈250 – 260 °C. As polymer **A** has a lower molar mass, M_n = 5.3 kDa and the cyanomethyl dodecyltrithiocarbonate RAFT agent has a molar mass of 317.6 Da; on average, ≈6 wt% of homopolymer **A** is the RAFT agent. Therefore, the ≈6 wt% mass loss which began at ≈250 – 260 °C for homopolymer **A** can be attributed to the thermal degradation of the RAFT end group. The thermal degradation of the RAFT end group is not as apparent for the higher molar mass polymers, **B** and **C**, as the weight percentage of the RAFT end group relative to the polymer is considerably lower. The thermal degradation of the RAFT end group at ≈250 – 260 °C was confirmed from the TGA curve for cyanomethyl dodecyltrithiocarbonate RAFT agent (Fig. S5) which indicates the onset of thermal

degradation for the RAFT agent occurs between ≈200-250 °C via thermal degradation mechanisms of the RAFT end groups and published previously in the literature.[50] In addition, the mass loss at 250-260 °C can contain a component from the decomposition of unreacted monomer. It is worth noting, the thermal degradation of the RAFT end group almost certainly leads to the production of free radicals which appears to not have a significant influence on the onset of degradation of the P[LA] backbone. Additionally, polymer **A** exhibits a shoulder at ≈370 – 380 °C which could possibly be attributed to the thermal degradation of an intermediary compound formed during the pyrolysis of the RAFT end group.[50] Importantly, P[LA] does not exhibit a radical induced 'unzipping' commonly seen with methacrylates such as, poly(methyl methacrylate) (PMMA) in which depolymerisation is observed at ≈ 300 °C.

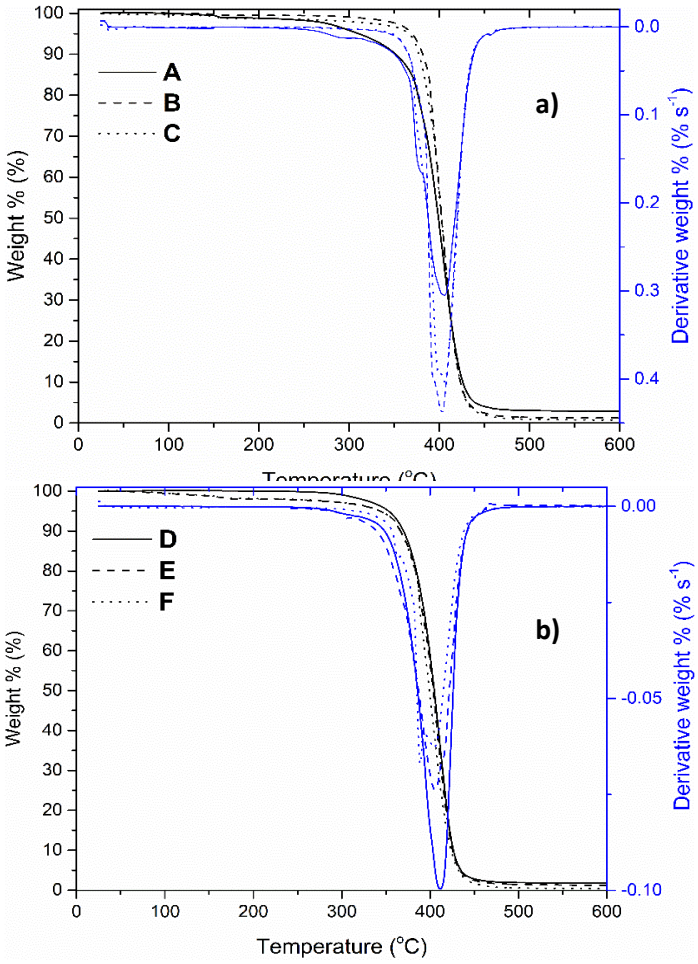

Fig. 3 TGA and DTA curves of P[LA] synthesised *via* (a) RAFT and (b) Cu(0) mediated polymerisation. P[LA] (**A-F**) defined in table 1 and 2.

The TGA data indicates P[LA] is sufficiently thermally stable for extrusion up to at least 250 °C and therefore, it should be possible to blend P[LA] with iPP for the purposes of improving MWCNT

dispersion and compatibility with the iPP matrix. It appears the thermal stability of P[LA] is not affected by the thermal decomposition of the RAFT end group.

P[LA] synthesised by Cu(0)-mediated polymerisation (Fig. 3b) has a similar thermal degradation profile to P[LA] synthesised by RAFT. The onset of thermal degradation occurs at ≈340-350 °C with 95% mass loss having occurred by 440-450 °C. Homopolymers **E** and **F** show a ≈2 – 3 wt% mass loss by 250 °C which could be attributed to the loss of unreacted monomer. The TGA of LA (Fig. S4) shows the onset of monomer degradation occurs at ≈140-150 °C. The data in Table 2 shows higher molar mass polymers **E** and **F** have lower conversions and therefore, unreacted monomer accounts for ≈2 – 3 wt% mass loss by 250 °C. A similar mass loss was also observed for P[LA] synthesised by RAFT. A shoulder placed between ≈290 – 300 °C indicates possible pyrolysis of end groups. It is possible the pyrolysis of the ethyl isobutyrate initiator occurs *via* an E_i (intramolecular elimination), also known as a thermal pericyclic *syn* elimination, to release ethylene[51]. In addition, the loss of the labile bromide end group can contribute to a total mass loss of ≈108 Da. On average, pyrolysis of the end groups could contribute a ≈2 wt% mass loss, for the lowest molar mass homopolymer **D**, resulting in the shoulder process observed between ≈290 – 300 °C.

Upon establishing the thermal stability of P[LA] is suitable for melt mixing with iPP, the interaction between P[LA] and MWCNTs was investigated. Initially, sonication and vigorous stirring was used to break up MWCNT agglomerates in a chloroform solution. Care was taken not to sonicate the MWCNTs for a prolonged period of time > 5 mins, as this can damage the structural integrity of MWCNTs. P[LA] was added to the dispersed MWCNT solutions, then briefly sonicated and vigorously stirred to allow adsorption of the polymer onto the MWCNT surfaces. (No evidence of tube damage was observed from extensive microscopic examination (SEM/HRTEM) across the length scales post sonication). The dispersion was subsequently filtered and dried. TGA was used to establish the amount of P[LA] adsorbed onto the surface of the MWCNTs. Table 3 lists the various P[LA]/MWCNT combinations and the relative ratios of P[LA] to MWCNTs before and after filtration (i.e. for the P[LA] synthesised using RAFT).

Table. 3 Relative proportions (wt%) of P[LA] (synthesised using RAFT) and MWCNTs before and after adsorption.

Nomenclature	P[LA]	Dispersion of P[LA]/MWCNT [a]		MWCNT adsorbed on P[LA][b]	
		P[LA]	MWCNT	MWCNT	P[LA]
A_5	A	95	5	88	12
A_{10}	A	90	10	84	16
B_5	B	95	5	79	21
B_{10}	B	90	10	86	14
C_5	C	95	5	81	19
C_{10}	C	90	10	78	22

[a] Dispersed in 100 ml $CHCl_3$. [b] TGA analysis of dried filter cake.

P[LA]s with three different degrees of polymerisation were chosen so as to investigate the effect of changing molar mass on the non-covalent wrapping/interaction with MWCNTs. After solution mixing P[LA] (synthesised by RAFT) with MWCNTs, the concentration of adsorption/coating was determined by TGA. Fig. 4a and Fig 4b show the TGA and DTA traces respectively, and indicate an adsorption of ≈10 - 25 wt% P[LA]. The onset of thermal degradation of P[LA] after adsorption appears to be unchanged at ≈340-350 °C. In general, the higher the molar mass of the P[LA], the greater the level of adsorption. This is expected due to one part of the polymer chain being adsorbed whilst, the remainder of the polymer chain is more likely to adsorb the CNT surface via CH-π interactions. The MWCNTs are thermally stable in the whole temperature range studied (up to 600 °C), with only negligible mass loss due to the presence of amorphous carbon and other impurities. Additionally, increasing the amount of MWCNTs results in P[LA] adsorption as the MWCNT surface area available is increased, thus more polymer is able to adsorb. Higher concentrations of P[LA] adsorption was expected and therefore, other factors, possibly bound solvent could be preventing adsorption of more P[LA].

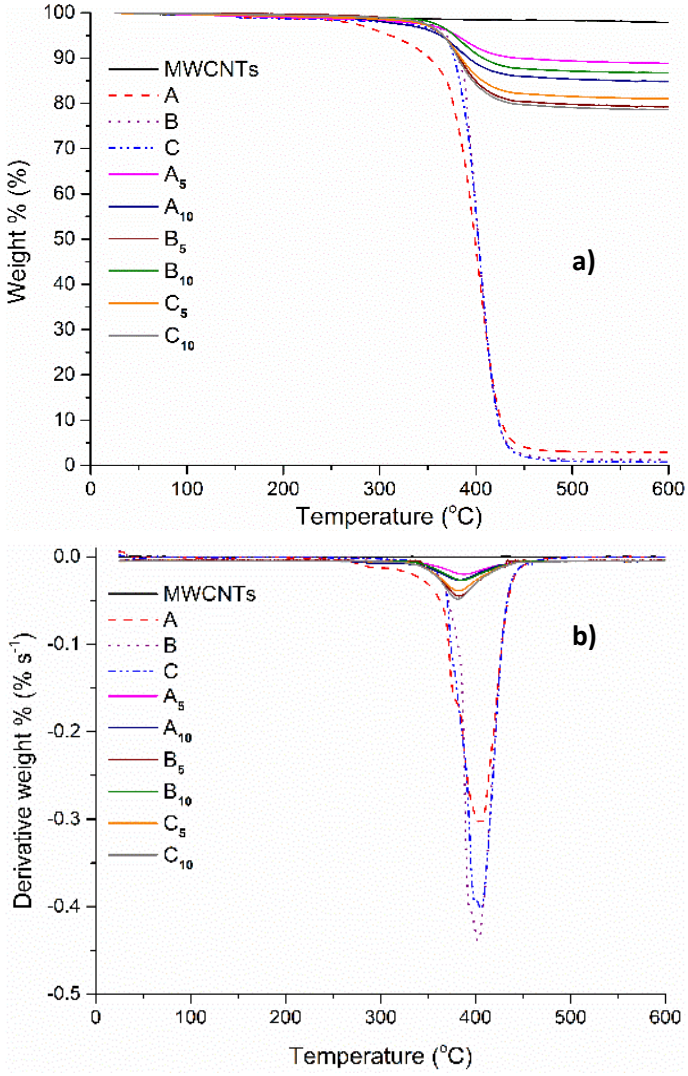

Fig. 4 (a) TGA weight loss curves and **(b)** DTA curves of P[LA] synthesised *via* RAFT and dispersed with MWCNTs. P[LA] (**A-C**) defined in table 1. P[LA] modified MWCNTs (**A-C**$_{(5/10)}$ defined in table 3.

Table 4 lists the various P[LA]/MWCNT combinations and the relative ratios of P[LA] to MWCNTs before and after filtration, (i.e. for P[LA] synthesised using Cu(0)-mediated polymerisation). The TGA curves of MWCNTs coated with P[LA] synthesised *via* Cu(0)-mediated polymerisation (Fig 5a and 5b) indicate a more enhanced interaction in that P[LA] synthesised by this method has increased thermal stability of ≈50 °C when adsorbed onto the surface of the MWCNTs and, a significantly greater concentration of this P[LA] adsorbs compared to P[LA] synthesised using RAFT. Un-bound P[LA] has a onset temperature for degradation of ≈340 - 350 °C, but P[LA] bound to the surface of the MWCNTs has a higher onset temperature of ≈400 – 410 °C.

Table. 4 Relative proportions (wt%) of P[LA] (synthesised using Cu(0)-mediated polymerisation) and MWCNTs before and after adsorption.

Nomenclature	P[LA]	Dispersion of P[LA]/MWCNTs[a]		MWCNTs adsorbed on P[LA][b]	
		P[LA]	MWCNT	MWCNT	P[LA]
D$_5$	D	95	5	86	14
D$_{10}$	D	90	10	83	17
E$_5$	E	95	5	65	35
E$_{10}$	E	90	10	42	58
F$_5$	F	95	5	16	84
F$_{10}$	F	90	10	67	33

[a] Dispersed in 100 ml $CHCl_3$. [b] TGA analysis of dried filter cake.

Additionally, a clear trend is observed where the higher the molar mass of the P[LA], the greater the concentration of P[LA] adsorbed. In general, the increase in concentration of MWCNTs also results in an increase in the concentration of P[LA] adsorption. These observations are in agreement with that reported above for the P[LA] synthesised using RAFT. The increased thermal stability of P[LA] (see Fig. 5a and 5b) confirms there is an interaction between the surface of the MWCNTs and the P[LA]. The increased thermal stability of P[LA] observed shows a interaction occurs between the surface of the MWCNTs and the P[LA]. However, it is unclear why this interaction is only observed with P[LA] synthesised by Cu(0)-mediated and not with RAFT. The difference in the thermal stability could be as a result of relative amounts of bound and un-bound P[LA]. It is possible the P[LA] synthesised by RAFT was adsorbed but poorly bound, however, the P[LA] synthesised by Cu(0)-mediated was bound. The free radicals produce by the P[LA] upon pyrolysis could have been quenched by the MWCNTs and hence delayed the radical catalysed pyrolysis of P[LA] normally observed at ≈340 - 350 °C and therefore, resulting in increased thermal stability. It is also possible P[LA] synthesised by Cu(0)-mediated reacts with the surface of MWCNTs which causes the delayed degradation of the polymer. Due to the fact LA polymerised by RAFT was carried out at higher temperatures, there is a greater degree of branching in the P[LA] synthesised by RAFT. The highly

branched structure could prevent the P[LA] from adsorbing as effectively compared to the more linear P[LA] synthesised by Cu(0)-methods.[52]

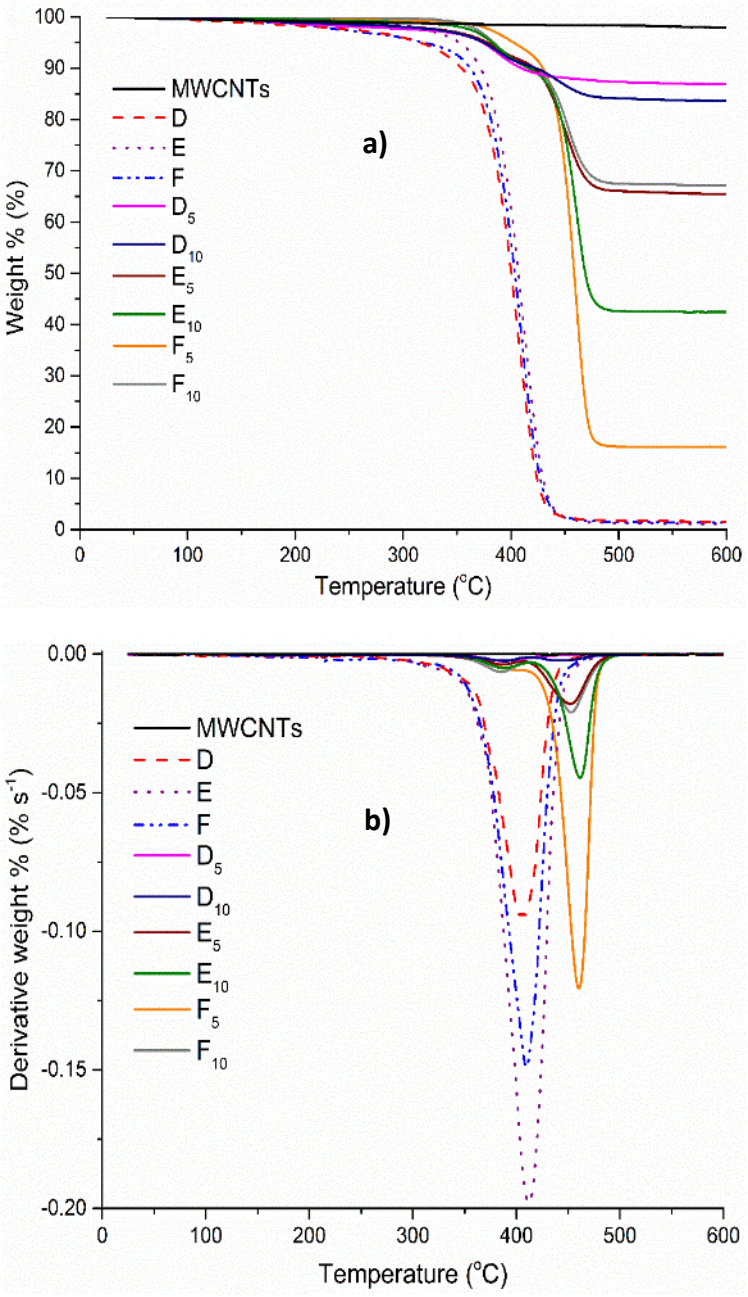

Fig. 5 (a) TGA weight loss curves of P[LA] synthesised *via* Cu(0) mediated polymerisation and P[LA] coated MWCNTs; (b) DTA curves of P[LA] synthesised *via* Cu(0) mediated polymerisation and P[LA] coated MWCNTs. P[LA] (**D-F**) defined in table 2. P[LA] modified MWCNTs (**D-F**$_{(5/10)}$ defined in table 4.

To further explore this difference in thermal degradation behaviour, molar mass analyses using SEC and MALDI-TOF-MS was performed on P[LA] synthesised by both RAFT and Cu(0) mediated methods, before and after heating to 200 °C for 30 mins in an air atmosphere.

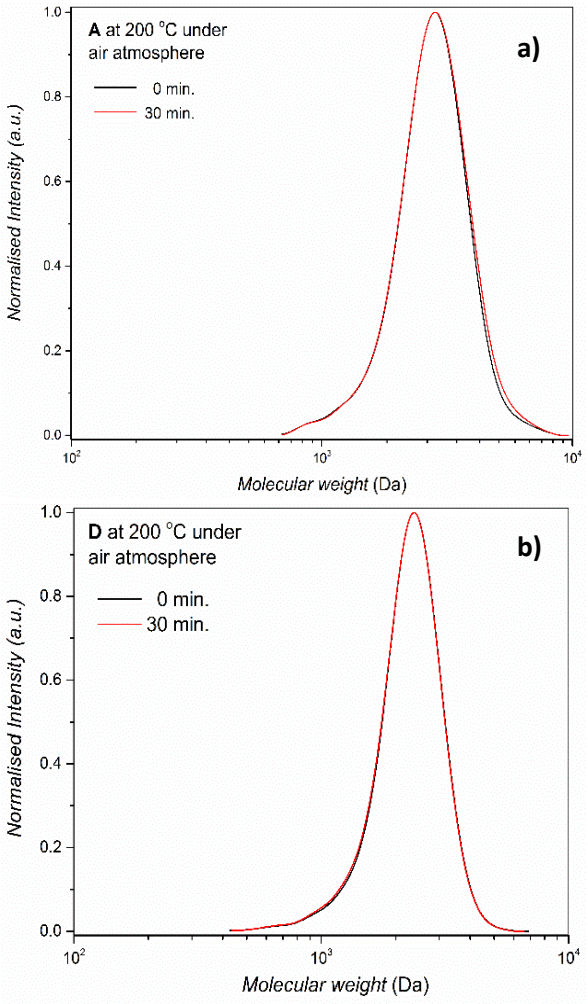

Fig. 6 SEC traces of P[LA] after thermal treatment at 200 °C under an air atmosphere as a function of time; (a) 0 min. ($M_{n,\,SEC}$ = 2.5 kDa, $Đ$ = 1.13), 30 min. ($M_{n,\,SEC}$ = 2.5 kDa, $Đ$ = 1.13); (b) 0 min. ($M_{n,\,SEC}$ = 2.1 kDa, $Đ$ = 1.11), 30 min. ($M_{n,\,SEC}$ = 2.1 kDa, $Đ$ = 1.11). All peaks are normalised to a maximum intensity of 1.

The effect of thermal treatment on the molar mass of the P[LA] was also investigated using SEC (Fig. 6). Limited if any, change in molar mass distribution was observed. This result confirms the end groups of both types of P[LA] do not affect the thermal stability of P[LA] and its potential use in melt processing.

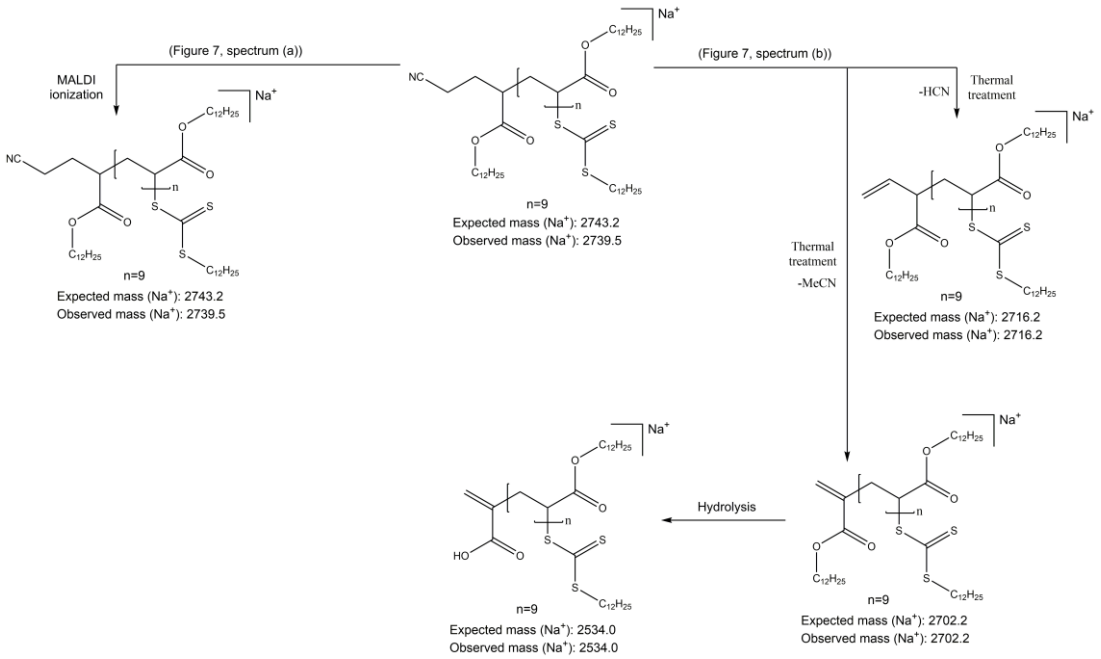

Scheme 4 Description of degradation products following the MALDI analysis of P[LA] synthesised *via* RAFT (a) before and (b) after thermal treatment (200 °C, 30 min.)

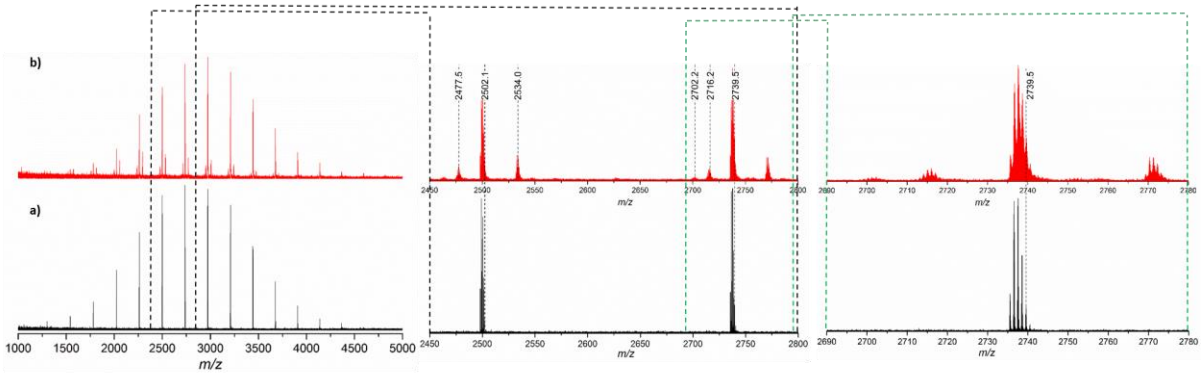

Fig. 7 MALDI-TOF-MS spectra of P[LA] synthesised *via* RAFT before (a) and after (b) thermal treatment at 200 °C for 30 mins in air..

MALDI-TOF-MS was used to further investigate the thermal characteristics of P[LA]. Fig. 7 clearly shows the molecular structure of P[LA] *via* RAFT changes when subjected to elevated temperatures, up to 200 °C. However, the repeating pattern of the peaks, separated by the relative molar mass of the monomer indicates the thermal degradation is not occurring at the polymer backbone. Possible structures for mass losses during degradation are described in scheme 4 and are in agreement with a recent report by Barner-Kowollik *et al*.[1] The main distributions are attributed to the polymer, *i.e. m/z* 2739 showing the majority of the polymer is unaffected by the thermal treatment. Mass loses at *m/z* 2702 and 2716 indicate the formation of an unsaturated species caused by the decomposition of the reactive nitrile group. Elimination of the nitrile group appears to have triggered the hydrolysis of a

nearby ester. The loss of lauryl alcohol and elimination of the reactive nitrile group is consistent with the signal at *m/z* at 2534. Interestingly, thermal decomposition of the RAFT group was not observed in the MALDI after thermal treatment suggesting the trithiocarbonate group and the polymer backbone is thermally stable at 200 °C for 30 min.

In addition, NMR (fig. S6) was used to confirm the formation of the unsaturated chain end after thermal treatment. Due to the relative concentration of the unsaturated chain end being very low compared with the polymer side-chain, detection of the chain end was not possible.

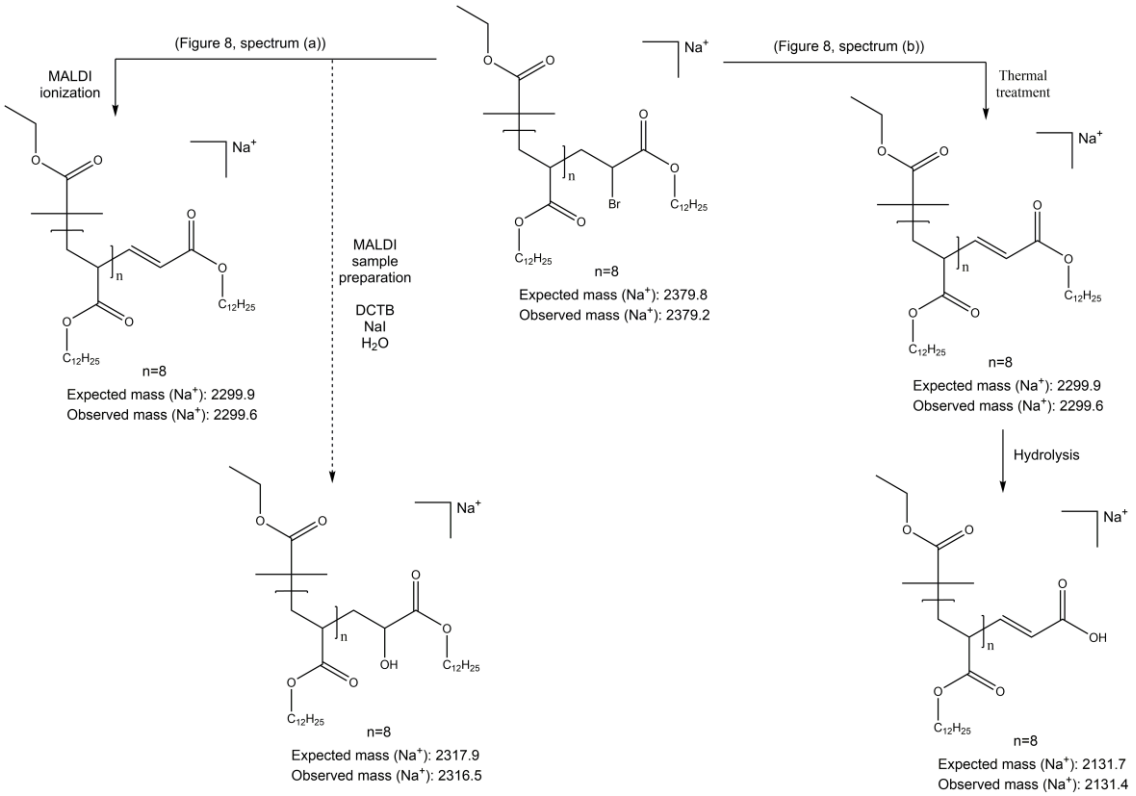

Scheme 5 Description of degradation products following the MALDI analysis of P[LA] synthesised *via* Cu(0)-mediated polymerisation (a) before and (b) after thermal treatment (200 °C, 30 min.)

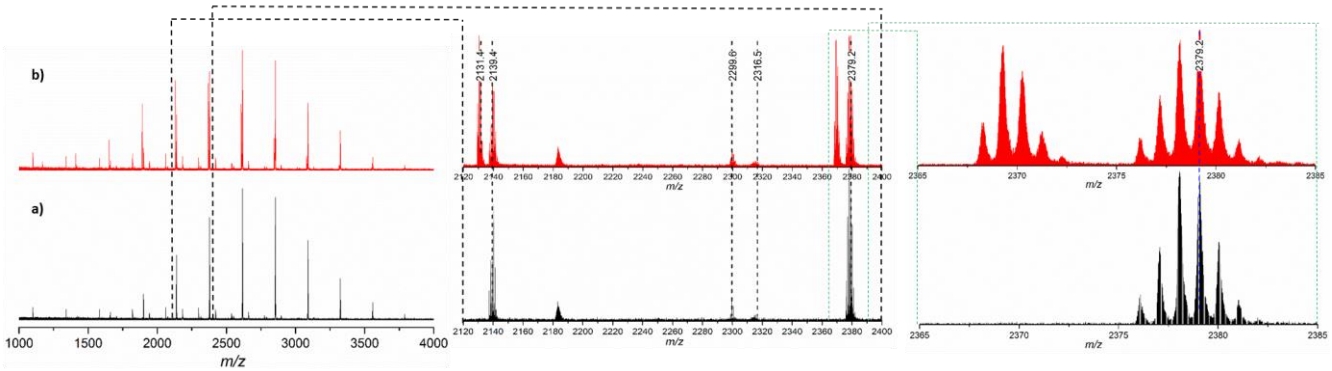

Fig 8. MALDI-TOF-MS spectra of P[LA] synthesised *via* Cu(0) mediated polymerisation before (a) and after (b) thermal treatment at 200 °C for 30 mins in air.

A similar experiment was repeated for P[LA] synthesised by Cu(0)-mediated polymerisation (Fig. 8). The mass loses observed are consistent with those reported by Barner-Kowollik *et al*.[1] Compared to the P[LA] synthesised by RAFT, ester hydrolysis is more apparent after the elimination of HBr. This is due to the acidic nature of HBr which causes increased hydrolysis compared with the nitrile group in the case of the RAFT polymer. Elimination of HBr and the possible substitution of a hydroxide moiety during the MALDI ionisation process was also observed for the acrylate polymers *i.e. m/z* 2299 and 2316. In addition, the subsequent hydrolysis of a nearby ester after elimination of HBr during thermal treatment is also in agreement with the recent report by Barner-Kowollik *et al*.[1] Identification of vinylic peaks at the end of the polymer chain was also attempted by NMR (fig. S7). Due to the relative concentration of the unsaturated chain end being very low compared the polymer side-chain, detection of the chain end was not possible.

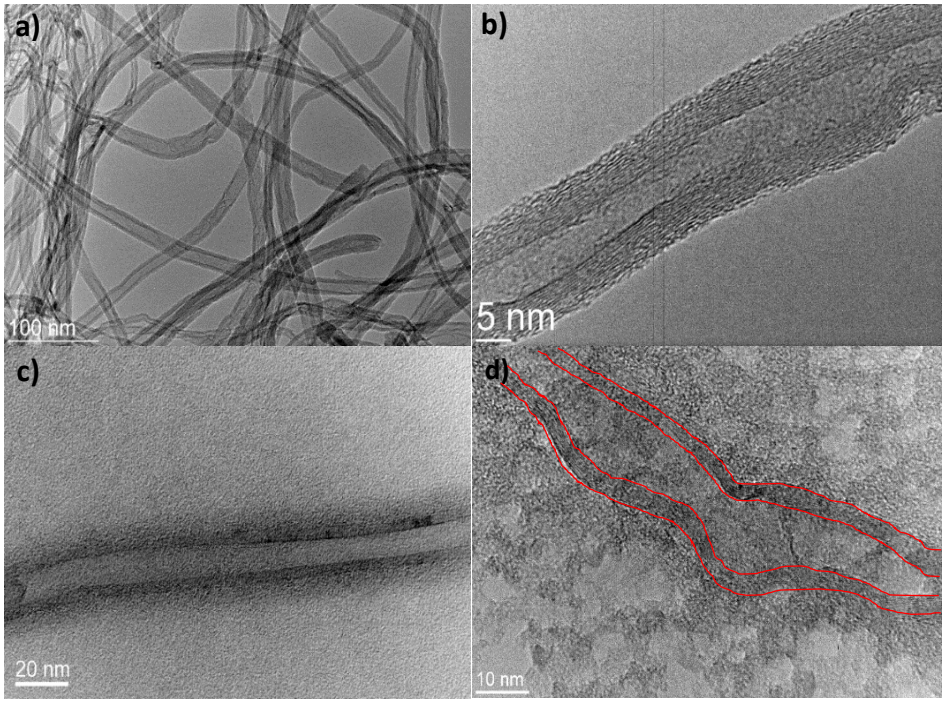

Fig 9. HRTEM images of (a) un-functionalised MWCNTs at 50k × magnification; (b) un-functionalised MWCNTs at 400k × magnification; (c) MWCNTs functionalised with P[LA] at 150k × magnification; (d) MWCNTs functionalised with P[LA] with red line to show inner and outer walls at 300k × magnification. (P[LA] polymerised via Cu(0)-mediated polymerisation).

Figure 9a and 9b show the uncoated MWCNTs at different magnifications, the entangled tube structure and multi-walled morphology can be observed. P[LA] chains adsorbed onto the surface of

MWCNTs can be seen due to the difference in phase contrast surrounding the MWCNTs in Figure 9c and 9d. The red lines (figure 9d) indicate the outer and inner walls of the MWCNTs and help to show the presence of P[LA] radiating from the outer wall of the MWCNT.

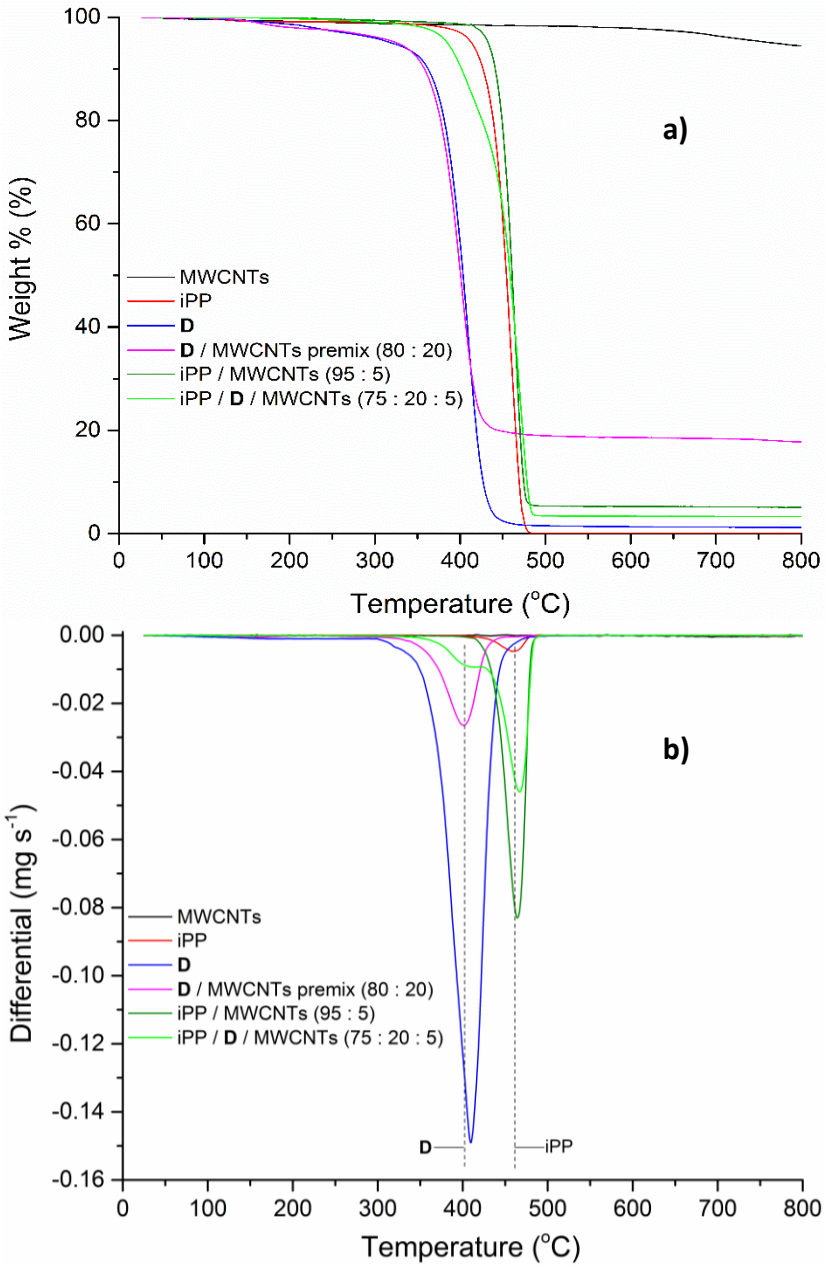

Fig 10. (a) TGA weight loss curves of MWCNTs premixed with P[LA] and melt mixed with iPP at 165 °C (b) DTA curves of MWCNTs premixed with P[LA] and melt mixed with iPP at 165 °C. P[LA] (**D**) defined in table 2.

P[LA](D) modified MWCNTs were melt mixed with iPP in an extruder (5 mins at 80 rpm and 165 °C) and the thermally stability of the composites prepared determined from TGA and DTA curves, see Fig 10. Interestingly, the thermal stability of iPP was increased on addition of MWCNTs, but that of P[LA](D) was unchanged. However, when all three components were melt mixed the thermal stability (below 460 °C) was intermediate between neat iPP and P[LA](D). Most importantly, the P[LA] component was thermally stable both during the extrusion cycle and via TGA post melt mixing.

Conclusion

The thermal and thermo-mechanical stability of P[LA] synthesised using RAFT and Cu(0)-mediated methods was determined. Its potential for MWCNT functionalisation and subsequent use in polymer processing with iPP was investigated.

P[LA] polymerised *via* a Cu(0)-mediated polymerisation method went to high monomer conversion (>98%), with the synthesised polymers in good agreement with theoretical M_n and low dispersity ($Đ$; ≈ 1.2). SEC analysis revealed a linear increase in molar mass with increasing monomer to initiator concentration for lower molar mass polymers. Low molar mass tailing was also observed for higher molar mass P[LA].

TGA analysis of P[LA] *via* RAFT showed the onset of thermal degradation occurred at ≈ 340 – 350 °C with 95% mass loss by ≈ 440 – 450 °C for higher molar mass P[LA]. Lower molar mass P[LA] exhibited a lower onset of thermal degradation at ≈ 250 – 260 °C caused by the thermal degradation of the RAFT end group, becoming more apparent at lower molar masses. The thermal degradation of the RAFT end group was confirmed from the TGA of the RAFT agent alone which had an onset between ≈ 200 – 250 °C.

TGA analysis of P[LA] *via* the Cu(0)-mediated method displayed a similar degradation profile to P[LA] *via* RAFT with the onset of degradation occurring at ≈ 340 – 350 °C. Higher molar mass P[LA] appeared to have a lower conversion which accounted for the ≈ 2 – 3 wt% mass loss by 250 °C due to loss of unreacted monomer. A shoulder placed between ≈ 290 – 300 °C indicated possible pyrolysis of end groups. The thermal stability of P[LA] is sufficient to make it readily processable with iPP.

TGA analysis indicated an adsorption of ≈ 10 – 25 wt% for P[LA] *via* RAFT on to the MWCNTs. Interestingly, P[LA] *via* Cu(0)-mediated polymerisation adsorbed at levels of up to ≈ 85 wt% and an increase in thermal stability of the P[LA] was recorded, by ≈ 50 °C when adsorbed onto the surface of the MWCNTs. The increase in thermal stability confirmed there are interactions

between P[LA] and the MWCNTs, possibly via CH-π. Radicals generated during pyrolysis could have possibly been quenched by the MWCNTs resulting in delayed radical catalysed pyrolysis of P[LA] *via* Cu(0)-mediated. The difference in thermal degradation observed between P[LA] synthesised by RAFT and Cu(0)-mediated could have possibly been due there being not enough P[LA] *via* RAFT being bound to the surface of the MWCNT for the quenching to become apparent. SEC analysis of P[LA] after heating to 200 °C under an air atmosphere for 30 mins, indicated the thermal degradation of the end groups did not alter the molar mass distribution of the P[LA]. MALDI-TOF-MS of P[LA] showed formation of unsaturated chain ends and subsequent hydrolysis of a nearby ester but, the polymer back-bone was unaffected for both polymerisation techniques.

Evidence from TEM micrographs confirmed the P[LA] chains were adsorbed onto the surface of MWCNTs. The presence of P[LA] radiating from the other wall of the MWCNT was shown due to the phase contrast surrounding the MWCNTs.

Upon processing P[LA](D) modified MWCNTs with iPP, the thermal stability of the composites were analysed using TGA post extrusion. P[LA] polymerised by both RAFT and Cu(0)-mediated readily interacts with MWCNTs and both are sufficiently thermally stable such they can be melt mixed with many engineering polymers, e.g. iPP. The compatibilisation effect and interaction between P[LA] and MWCNTs on the properties of iPP is currently under investigation and will be reported shortly.

Acknowledgements

We acknowledge support from Anish Mistry for HR ESI-MS, Athina Anastasaki for MALDI-TOF and Martin Worrall for technical assistance.

References

1. O. Altintas, T. Josse, M. Abbasi, J. De Winter, V. Trouillet, P. Gerbaux, M. Wilhelm and C. Barner-Kowollik, *Polym. Chem.*, 2015, **6**, 2854-2868.
2. O. Altintas, T. Josse, J. De Winter, N. M. Matsumoto, P. Gerbaux, M. Wilhelm and C. Barner-Kowollik, *Polym. Chem.*, 2015, **6**, 6931-6935.
3. W. A. Braunecker and K. Matyjaszewski, *Prog. Polym. Sci.*, 2007, **32**, 93-146.
4. K. Matyjaszewski and J. H. Xia, *Chem. Rev.*, 2001, **101**, 2921-2990.
5. C. J. Hawker, A. W. Bosman and E. Harth, *Chem. Rev.*, 2001, **101**, 3661-3688.
6. R. T. A. Mayadunne, E. Rizzardo, J. Chiefari, Y. K. Chong, G. Moad and S. H. Thang, *Macromolecules*, 1999, **32**, 6977-6980.

7. D. J. Keddie, *Chem. Soc. Rev.*, 2014, **43**, 496-505.
8. G. Moad, E. Rizzardo and S. H. Thang, *Aust. J. Chem.*, 2009, **62**, 1402-1472.
9. S. Perrier and P. Takolpuckdee, *J. Polym. Sci., Part A: Polym. Chem.*, 2005, **43**, 5347-5393.
10. Q. Zhang, P. Wilson, Z. D. Li, R. McHale, J. Godfrey, A. Anastasaki, C. Waldron and D. M. Haddleton, *J. Am. Chem. Soc.*, 2013, **135**, 7355-7363.
11. B. M. Rosen and V. Percec, *Chem. Rev.*, 2009, **109**, 5069-5119.
12. A. Anastasaki, V. Nikolaou and D. M. Haddleton, *Polym. Chem.*, 2016, **7**, 1002-1026.
13. A. Anastasaki, V. Nikolaou, A. Simula, J. Godfrey, M. X. Li, G. Nurumbetov, P. Wilson and D. M. Haddleton, *Macromolecules*, 2014, **47**, 3852-3859.
14. C. Waldron, A. Anastasaki, R. McHale, P. Wilson, Z. D. Li, T. Smith and D. M. Haddleton, *Polym. Chem.*, 2014, **5**, 892-898.
15. K. Matyjaszewski, *Macromolecules*, 2012, **45**, 4015-4039.
16. D. J. Keddie, G. Moad, E. Rizzardo and S. H. Thang, *Macromolecules*, 2012, **45**, 5321-5342.
17. B. Chong, G. Moad, E. Rizzardo, M. Skidmore and S. H. Thang, *Aust. J. Chem.*, 2006, **59**, 755-762.
18. A. Postma, T. P. Davis, G. Moad and M. S. O'Shea, *Macromolecules*, 2005, **38**, 5371-5374.
19. O. Altintas, K. Riazi, R. Lee, C. Y. Lin, M. L. Coote, M. Wilhelm and C. Barner-Kowollik, *Macromolecules*, 2013, **46**, 8079-8091.
20. O. Altintas, M. Abbasi, K. Riazi, A. S. Goldmann, N. Dingenouts, M. Wilhelm and C. Barner-Kowollik, *Polym. Chem.*, 2014, **5**, 5009-5019.
21. S. Iijima, *Nature*, 1991, **354**, 56-58.
22. A. Jorio, M. S. Dresselhaus and G. Dresselhaus, *Carbon Nanotubes: Advanced Topics in the Synthesis, Structure, Properties and Applications*, Springer, Heidelberg, 2008.
23. E. T. Thostenson, Z. F. Ren and T. W. Chou, *Compos. Sci. Technol.*, 2001, **61**, 1899-1912.
24. G. Pandey and E. T. Thostenson, *Polymer. Rev.*, 2012, **52**, 355-416.
25. T. Fujigaya and N. Nakashima, *Sci. Technol. Adv. Mater.*, 2015, **16**, 1-21.
26. J. H. Du, J. Bai and H. M. Cheng, *Express. Polym. Lett.*, 2007, **1**, 253-273.
27. A. E. Daugaard, K. Jankova and S. Hvilsted, *Polymer*, 2014, **55**, 481-487.
28. Y. P. Sun, K. F. Fu, Y. Lin and W. J. Huang, *Acc. Chem. Res.*, 2002, **35**, 1096-1104.
29. S. H. Qin, D. Q. Oin, W. T. Ford, D. E. Resasco and J. E. Herrera, *J. Am. Chem. Soc.*, 2004, **126**, 170-176.
30. W. Wu, N. V. Tsarevsky, J. L. Hudson, J. M. Tour, K. Matyjaszewski and T. Kowalewski, *Small*, 2007, **3**, 1803-1810.
31. G. Clave and S. Campidelli, *Chem. Sci.*, 2011, **2**, 1887-1896.
32. D. A. Britz and A. N. Khlobystov, *Chem. Soc. Rev.*, 2006, **35**, 637-659.
33. Y. L. Zhao and J. F. Stoddart, *Acc. Chem. Res.*, 2009, **42**, 1161-1171.
34. S. Meuer, L. Braun and R. Zentel, *Macromol. Chem. Phys.*, 2009, **210**, 1528-1535.
35. N. Karousis, N. Tagmatarchis and D. Tasis, *Chem. Rev.*, 2010, **110**, 5366-5397.
36. P. Bilalis, D. Katsigiannopoulos, A. Avgeropoulos and G. Sakellariou, *RSC. Adv.*, 2014, **4**, 2911-2934.
37. C. F. Yu, Q. Chen, A. Q. Wang, X. Zhou, S. S. Wu and Q. P. Ran, *Polym. Int.*, 2015, **64**, 1219-1224.
38. S. W. Kim, T. Kim, Y. S. Kim, H. S. Choi, H. J. Lim, S. J. Yang and C. R. Park, *Carbon*, 2012, **50**, 3-33.
39. A. Anastasaki, C. Waldron, V. Nikolaou, P. Wilson, R. McHale, T. Smith and D. M. Haddleton, *Polym. Chem.*, 2013, **4**, 4113-4119.
40. J. Y. T. Chong, D. J. Keddie, A. Postma, X. Mulet, B. J. Boyd and C. J. Drummond, *Colloids Surf., A*, 2015, **470**, 60-69.
41. J. D. Moskowitz and J. S. Wiggins, *Polym. Degrad. Stab.*, 2016, **125**, 76-86.

42. G. Moad, G. Li, R. Pfaendner, A. Postma, E. Rizzardo, S. Thang and H. Wermter, in *Controlled/Living Radical Polymerization*, ed. K. Matyjaszewski, American Chemical Society, 2006, vol. 944, ch. 35, pp. 514-532.
43. M. Ciampolini and N. Nardi, *Inorg. Chem.*, 1966, **5**, 41-44.
44. B. Krause, M. Mende, P. Pötschke and G. Petzold, *Carbon*, 2010, **48**, 2746-2754.
45. B. Krause, T. Villmow, R. Boldt, M. Mende, G. Petzold and P. Pötschke, *Compos. Sci. Technol.*, 2011, **71**, 1145-1153.
46. Y. K. Chong, G. Moad, E. Rizzardo and S. H. Thang, *Macromolecules*, 2007, **40**, 4446-4455.
47. J. Y. T. Chong, X. Mulet, A. Postma, D. J. Keddie, L. J. Waddington, B. J. Boyd and C. J. Drummond, *Soft Matter*, 2014, **10**, 6666-6676.
48. D. J. Keddie, C. Guerrero-Sanchez, G. Moad, R. J. Mulder, E. Rizzardo and S. H. Thang, *Macromolecules*, 2012, **45**, 4205-4215.
49. K. L. Chen, Y. H. Zhao and X. Y. Yuan, *Chem. Res. Chin. Univ.*, 2014, **30**, 339-342.
50. H. Willcock and R. K. O'Reilly, *Polym. Chem.*, 2010, **1**, 149-157.
51. J. Clayden, N. Greeves, S. Warren and P. Wothers, in *Organic Chemistry*, ed. J. Clayden, Oxford University Press, Oxford, UK, 1st edn., 2001, ch. 38, pp. 1013-1014.
52. M. Gaborieau, S. P. S. Koo, P. Castignolles, T. Junkers and C. Barner-Kowollik, *Macromolecules*, 2010, **43**, 5492-5495.